

Chemokine and Cytokine Mediated Loss of Regulatory T Cells in Lymph Nodes during Pathogenic Simian Immunodeficiency Virus Infection¹

Shulin Qin,^{2*} Yongjun Sui,^{2*} Adam C. Soloff,^{*†} Beth A. Fallert Junecko,^{*} Denise E. Kirschner,^{||} Michael A. Murphey-Corb,[‡] Simon C. Watkins,[§] Patrick M. Tarwater,[#] James E. Pease,^{**} Simon M. Barratt-Boyes,^{*†||} and Todd A. Reinhart^{3*}

Regulatory T cells (T_{reg}) play key roles in immune regulation through multiple modes of suppression. The effects of HIV-1 infection on T_{reg} levels in lymphoid tissues remain incompletely understood. To explore this issue, we have measured the levels of forkhead box protein 3 (FOXP3)-positive cells and associated immunomodulatory genes in a pathogenic simian immunodeficiency virus/macaque model and found that a loss of T_{reg} in lymph nodes occurred following simian immunodeficiency virus infection. Changes in expression of the ligands for CXCR3, CCR4, and CCR7 and the cytokines TGF- β and IL-2 were all linked to this loss of T_{reg}, which in turn was linked with increased levels of cellular activation. Our findings identify three mechanisms that likely contribute to SIV-driven loss of T_{reg}, including reduced levels of cytokines associated with T_{reg} differentiation and altered expression of agonist and antagonist chemokines. The loss of T_{reg} and the associated cellular activation in lymphoid tissues is consistent with the events in HIV-1-infected individuals and suggest that components of the T_{reg} differentiation and trafficking network could be targets for therapeutic intervention. *The Journal of Immunology*, 2008, 180: 5530–5536.

Regulatory T cells (T_{reg})⁴ play important roles in the regulation of innate and acquired immunity through multiple modes of suppression. These cells contribute to control of autoimmunity as well as suppression of virus- and tumor-specific immune responses (1, 2). The transcription factor forkhead box protein 3 (FOXP3) is considered to be a highly specific marker for T_{reg} and is a key regulatory gene for their development (3). Increasing evidence indicates that cytokines are involved in regulation of T_{reg}. For example, TGF- β 1 and IL-2 are important for differentiation, expansion, and survival of FOXP3⁺ T_{reg}, because both cytokines can induce FOXP3 expression and FOXP3⁺ T_{reg} suppressive activity (4). Recent reports have indicated that chemokine receptors CCR4 and CCR7 are important in T_{reg} homing to lymph nodes (LNs) and other tissues (5, 6). Indeed, human T_{reg}

highly express CCR4 (7) and CCR7 (5), and thus their ligands CCL17 and CCL21 could modulate homing of T_{reg} to lymphoid tissues. Chemokines are small chemoattractant cytokines that orchestrate leukocyte migration during inflammation and as part of homeostatic immune function, and increasing evidence demonstrates that HIV-1 and simian immunodeficiency virus (SIV) infection lead to remodeling of chemotactic environments in lymphoid tissues (8, 9).

Chronic states of T cell hyperactivation, viral persistence, and CD4⁺ T cell depletion are hallmarks of HIV-1 infection (10), and the roles played by T_{reg} in this complex set of events remain unclear (11, 12). Decreased levels of T_{reg} during HIV-1 infection could lead to development of hyperactivated immune environments, increased viral replication, and activation-associated cell death, whereas increased levels of T_{reg} could lead to suppression of HIV-1-specific and other immune responses. The effects of HIV-1 infection on T_{reg} levels in lymphoid tissues remain incompletely understood and there are multiple reports in the literature that T_{reg} levels increase or decrease during HIV-1 or SIV infection (13–17), but the mechanisms that lead to alteration of T_{reg} levels in lymphoid tissues after HIV-1 or SIV infection have not been well defined. In the present study, we investigated the effects of pathogenic SIV infection on T_{reg} levels. Our findings indicate that there is a loss of T_{reg} in LNs following pathogenic SIV infection that is linked with changes in expression of the ligands for CXCR3, CCR4, and CCR7 and the cytokines TGF- β and IL-2.

Materials and Methods

Animals and tissues

These studies were performed under the approval and guidance of the University of Pittsburgh Institutional Animal Care and Use Committee. They included 12 cynomolgus macaques (*Macaca fascicularis*) infected with SIV/DeltaB670 (18). Of these animals, six were sacrificed during acute infection (2 wk postinfection (PI)), five were sacrificed upon progression to AIDS, and five served as uninfected controls. Details regarding tissue processing and fixation have been previously described (8).

*Department of Infectious Diseases and Microbiology, Graduate School of Public Health, [†]Center for Vaccine Research, [‡]Department of Molecular Genetics and Biochemistry, [§]Department of Cell Biology and Physiology, and ^{||}Department of Immunology, School of Medicine, University of Pittsburgh, Pittsburgh, PA 15260; ^{||}Department of Microbiology and Immunology, University of Michigan, Ann Arbor, MI 48109; [#]Departments of Biostatistics and Epidemiology, University of Texas Health Science Center, Houston, TX 77030; and ^{**}Leukocyte Biology Section, National Heart and Lung Institute, Faculty of Medicine, Imperial College London, London, United Kingdom

Received for publication January 7, 2008. Accepted for publication February 8, 2008.

The costs of publication of this article were defrayed in part by the payment of page charges. This article must therefore be hereby marked *advertisement* in accordance with 18 U.S.C. Section 1734 solely to indicate this fact.

¹ This work was supported by Public Health Service Grants AI060422 (to T.A.R.), HL072682 (to D.E.K.), and U54 RR02241 (to S.C.W.).

² S.Q. and Y.S. contributed equally to this work.

³ Address correspondence and reprint requests to Dr. Todd A. Reinhart, Department of Infectious Diseases and Microbiology, Graduate School of Public Health, University of Pittsburgh, 606 Parran Hall, 130 DeSoto Street, Pittsburgh, PA 15261. E-mail address: reinhar@pitt.edu

⁴ Abbreviations used in this paper: T_{reg}, regulatory T cell; LN, lymph node; SIV, simian immunodeficiency virus; PI, postinfection; FOXP3, forkhead box protein P3.

Table I. Study animals and clinicovirologic states

Animal	Stage	Virus ^a	Week PI	Plasma Viral Load ^b (copies/ml)	Axillary LN Viral Load ^c	Clinical State
M5602	Uninfected	None	0	ND	<0.01	No clinical symptoms
M6202	Uninfected	None	0	ND	<0.01	No clinical symptoms
M6802	Uninfected	None	0	ND	<0.01	No clinical symptoms
M7102	Uninfected	None	0	ND	<0.01	No clinical symptoms
M13402	Uninfected	None	0	ND	<0.01	No clinical symptoms
M13502	Uninfected	None	0	ND	<0.01	No clinical symptoms
M7802 ^d	Exposed/uninfected	SIV ^e	2	<10	<0.01	No clinical symptoms
M6002	Acute infection	SIV	2	2,600,000	76.9	No clinical symptoms
M7902	Acute infection	SIV	2	3,100,000	56.3	No clinical symptoms
M8002	Acute infection	SIV	2	1,450,000	7.6	No clinical symptoms
M13202	Acute infection	SIV	2	41,300,000	6.6	No clinical symptoms
M19102	Acute infection	SIV	2	380,000,000	28.2	No clinical symptoms
M5802	AIDS	SIV	49	1,950,000	17.8	Weight loss, CD4 ⁺ T cell loss
M6302	AIDS	SIV	80	<10 ^f	12.3	CD4 ⁺ T cell loss
M7002	AIDS	SIV	48	640,000	15.3	Weight loss, CD4 ⁺ T cell loss, diarrhea
M7602	AIDS	SIV	84	36,000	3.6	Anorexia, diarrhea, epistaxis
M12402	AIDS	SIV	42	50,500	3.5	Weight loss, CD4 ⁺ T cell loss, <i>Pneumocystis carinii</i> pneumonia

^a Intrarectal inoculation.

^b Real-time RT-PCR was used to determine plasma viral loads at necropsy.

^c Real-time RT-PCR was used to determine tissue-associated viral loads, with normalization to the copy numbers of β_2 -microglobulin mRNA (\times 1000).

^d SIV was not detectable in plasma nor in axillary LN samples for this animal.

^e SIV is SIV/DeltaB670.

^f Despite repeating the assay twice, viral RNA was unexpectedly not detected in this plasma sample.

RNA isolation and real-time RT-PCR

Total RNAs from axillary LNs were isolated, treated with DNase (Ambion), and further purified with RNeasy columns (Qiagen) as described previously (19). Four hundred nanograms of RNA from each specimen was reverse transcribed as previously described (19), with reverse transcriptase-negative controls included in parallel for each RNA sample. Primers and probes used for the real-time RT-PCR were either purchased from Applied Biosystems as ready-made sets or were designed using the Primer Express (Applied Biosystems) software package (primer and probe sequences that we designed are available upon request). Real-time RT-PCR was used to measure relative mRNA expression levels by the comparative threshold cycle method of relative quantitation as described elsewhere (19, 20). The threshold cycle values for each gene were normalized to the endogenous control mRNA β -glucuronidase and then to an uninfected LN calibrator sample. Quantitation of tissue-associated SIV viral loads was performed as described elsewhere (19).

Immunofluorescence staining and quantitative image analysis

Two-color immunofluorescence staining was performed by incubating tissue sections simultaneously with either anti-FOXP3 (Abcam) or anti-Ki67 (DakoCytomation) Abs at a 1/50 dilution along with anti-CD3 (Dako Cytomation) Ab at a 1/100 dilution, subsequently incubating with fluorescein- and biotin-SP (Jackson ImmunoResearch Laboratories)-conjugated secondary Abs, followed by the tertiary conjugates Alexa Fluor 488-anti-FITC and Alexa Fluor 647-streptavidin (Molecular Probes). Following signal intensification of the FITC signal (Molecular Probes) and nuclear staining with Sytox Orange (Molecular Probes), sections were treated with Autofluorescence Eliminator (Chemicon International) before mounting with Prolong Gold Antifade (Molecular Probes). Laser scanning confocal microscopy was performed with an Olympus FluoView 500 confocal microscope through a $\times 40$ objective, and images were obtained from sections simultaneously stained for Ki67 and CD3 or FOXP3 and CD3. Five random images were obtained throughout each section stained for Ki67 and CD3 and five random images were taken specifically from the paracortex of each section stained for FOXP3 and CD3. Quantitative image analysis was performed on these images using the MetaMorph software package (Molecular Devices). A journal was written and used to open each image, separate the fluorophore-specific signals, and then change the images to monochrome. Background shading and correction was used to flatten the background of the image of all nuclei stained with Sytox Orange and then autothresholding was performed for light objects. A low-pass filter was applied and the image was manually thresholded, binarized, and segmented. The image that contained cells stained with FITC (Ki67 or FOXP3) was also subjected to flatten background, low-pass filter, and

thresholding actions. The "holes" morphological filter was used to fill dark holes in the centers of cells. The images containing cells stained with Alexa Fluor 647 (CD3) were subjected to the same operations as the FITC images, with an additional binary operation added at the end to erode the image. We then used arithmetic AND-minimum functions to combine the images to count all cells and singly and doubly stained cells. Integrated morphometry analysis was used to count the individual Ki67⁺, FOXP3⁺, or CD3⁺ cells and double-positive cells (Ki67⁺CD3⁺ or FOXP3⁺CD3⁺) for each image. Ki67⁺CD3⁺ cell or FOXP3⁺CD3⁺ percentages were calculated from five images.

Immunohistochemistry and immunocytochemistry

Immunohistochemical staining of LN tissue sections was performed as described previously (8, 19) using goat anti-CCR4 polyclonal antiserum (Abcam) or preimmune control serum (BD Biosciences). After washing in PBS twice, tissue sections were incubated with HRP-conjugated secondary Ab (Zymed Laboratories) for 15 min, and 3,3'-diaminobenzidine substrate in Tris buffer was used for the detection of CCR4⁺ cells. Immunocytochemistry was performed for detection of FOXP3 in cells spotted onto microscope slides after in vitro chemotaxis. The cells examined by chemotaxis were uninfected cynomolgus macaque LN cells that migrated in response to chemokines (PeproTech) using an established chemotaxis assay (21). Spotted cells were stained with an anti-FOXP3 mAb (clone 234A/E7; Abcam). The numbers of FOXP3⁺ cells were determined by counting total and FOXP3⁺ cells in five low-powered microscopic fields ($\times 200$).

Generation of macaque lymphoid tissue single-cell suspensions

Lymphoid tissues from cynomolgus macaques were minced in digestion medium (RPMI 1640) containing DNase I (20 mg/ml; Sigma-Aldrich) and collagenase A (1 mg/ml; Roche) for 60 min at 37°C, passed through a 100- μ m cell strainer, and pelleted by centrifugation at 1200 rpm for 5 min. The pellet was resuspended in 1 \times RBC lysing solution (155 mM NH₄Cl, 10 mM NaHCO₃, and 0.1 mM EDTA, pH 7.4) for 5 min and centrifuged again at 1200 rpm for 5 min. The resulting cell pellet was resuspended in 1 \times PBS, counted on a hemacytometer, and aliquots of cell suspensions were frozen in freezing medium (90% FCS and 10% DMSO) and stored in liquid nitrogen. Gently thawed cells were exposed to rIFN- γ (50 ng/ml; R&D Systems), or medium alone, and total RNAs were isolated at 24 or 48 h later. Real-time RT-PCR was performed to measure chemokine or chemokine receptor mRNA levels as described elsewhere (19).

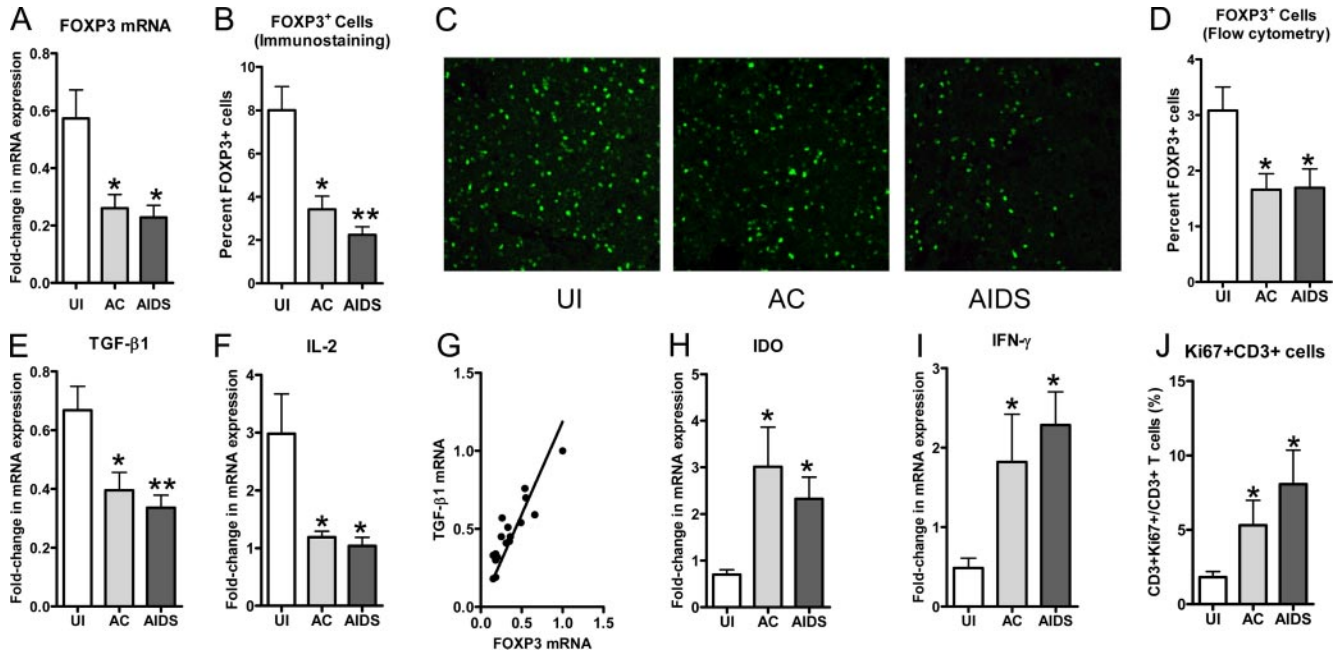


FIGURE 1. Changes in FOXP3 and cytokine levels in LN tissues during SIV infection of cynomolgus macaques. *A*, Real-time RT-PCR was used for measurement of FOXP3 mRNA in LN tissues from uninfected macaques or macaques in the early (acute (AC)) or late (AIDS) stages of disease (mean \pm SEM). Immunofluorescence staining was performed to detect (*C*; original magnification, $\times 400$) and quantitate (*B*) FOXP3⁺ cells in axillary LN tissue sections. *D*, Flow cytometry was used to detect and quantitate the percentage of total live cells that expressed FOXP3⁺ in the same LNs. *E*, *F*, *H*, and *I*, The relative levels of expression of the indicated mRNAs in macaque axillary LNs were examined by real-time RT-PCR (mean \pm SEM). *G*, Linear regression of FOXP3 mRNA levels vs TGF- β mRNA levels is shown. *J*, Quantitative image analysis was performed on images from LN tissue sections immunostained simultaneously for CD3 and the proliferation marker Ki67 and the percentages of CD3⁺ cells that were also Ki67⁺ are shown. *, $p < 0.05$ and **, $p < 0.01$, compared with uninfected animals.

Flow cytometric analysis

Anti-human mAbs were prescreened using multiple clonal and fluorometric combinations and selected on their ability to optimally discriminate antigenic expression by cynomolgus macaque LN cells. Live T cells were identified through successive gating strategies based on

size and viability using the blue LiveDead apoptotic stain (Molecular Probes/Invitrogen Life Technologies). Immunophenotyping of extracellular T_{reg} markers and chemokine receptors was performed on single-cell LN suspensions using the following Abs (purchased from BD Pharmingen, unless otherwise noted): CD3-Pacific Blue (SP34-2),

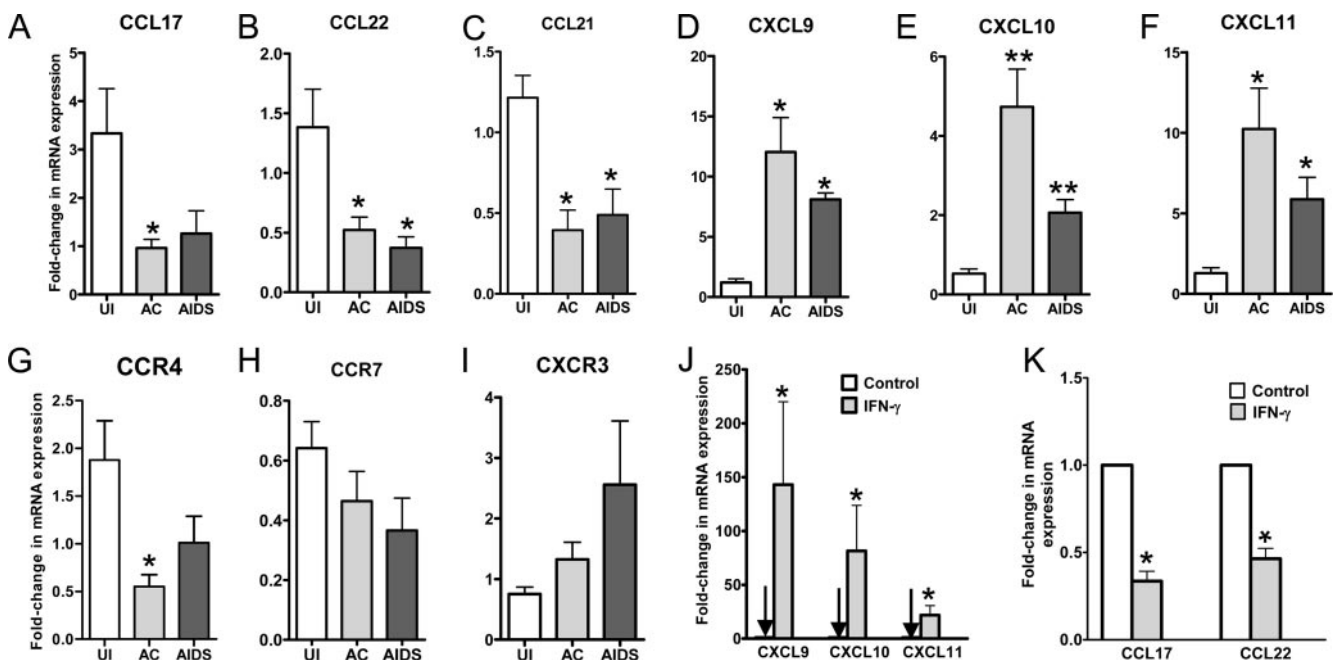


FIGURE 2. Changes in the relative expression levels of chemokine and chemokine receptor mRNAs during pathogenic SIV infection. *A–I*, Real-time RT-PCR was used to measure the levels of expression of the indicated mRNA in LNs from animals in the same disease states as described in the legend to Fig. 1. *J* and *K*, The effects of IFN- γ treatment of cynomolgus macaque primary LN cells on mRNAs encoding ligands for CXCR3 and CCR4 were measured using real-time RT-PCR. The mean (\pm SEM) values are shown from analyses performed on cells from three different animal. *, $p < 0.05$ and **, $p < 0.01$.

CD4-AmCyan (L200; National Institutes of Health Nonhuman Primate Reagent Resource Program, Boston, MA.), CD8-allophycocyanin-Cy7 (RPA-T8), and CD25-PE-Cy7 (M-A251) and CXCR3-PE (1C6/CXCR3), CCR4-PE (1G1), CCR6-PE (11A9), and CCR7-PE (150503; R&D Systems). Cryopreserved cells were thawed, washed, and stained for surface markers for 1 h at 4°C. Fixation and intracellular staining was performed with BD Biosciences Fix/Perm reagent kits according to the BD Biosciences protocol. Upon permeabilization, cells were stained intracellularly for FoxP3-FITC (236A/E7; eBioscience) for 1 h at 4°C. Appropriate isotype controls were included in all experiments. Data acquisition was performed on a LSRII cytometer housed at the University of Pittsburgh's Center for Vaccine Research with a minimum of 200,000 events collected from each sample. Data were analyzed using BD FACSDiva software (BD Biosciences).

Cell transfection and chemotaxis assays

A human CCR4 cDNA in the pcDNA3.1 vector was obtained from the University of Missouri cDNA Resource Center. Cell transfections were performed as described previously (21). Briefly, the L1.2 murine pre-B cell line was electroporated with pcDNA3.1 (Invitrogen Life Technologies) expressing human CCR4, and stably transfected cells were obtained after selection with 1 mg/ml G418 (Sigma-Aldrich). Chemotaxis was performed against CCL17 (10 μ M) with or without coinubation with CXCL11 or CXCL8 (100 μ M each). The 96-well ChemoTx chemotaxis system (5- μ m pore; NeuroProbe) was used for these chemotaxis assays and chemokines were obtained from PeproTech. The lower wells were blocked with 31 μ l of RPMI 1640/1% BSA for 30 min at room temperature, which was aspirated and replaced with 31 μ l of the agonists, which were diluted in RPMI 1640/0.1% BSA. Then 2×10^5 CCR4 stably transfected L1.2 cells in 20 μ l of RPMI 1640/0.1% BSA were loaded above the membrane. After incubation for 5 h at 37°C in 5% CO₂, the cells on top of the membrane were removed with a scraper and the migrated cells in the bottom wells were counted using a hemocytometer. Chemotaxis with macaque LN cells was performed in the same way, but with a 1.5-h incubation during migration.

Statistical analyses

All statistical analyses were performed using the Minitab software package (State College). Real-time RT-PCR data were analyzed using the two-sample *t* test to compare differences between disease states and Pearson's correlation analyses were used to measure associations between relative mRNA expression levels. Paired *t* tests were used to examine the chemotaxis inhibition data. A *p* < 0.05 was considered significant.

Results

To determine whether pathogenic SIV infection affects T_{reg} proportions in lymphoid tissues, we used a cynomolgus macaque (*M. fascicularis*) model and examined tissues at different stages after intrarectal infection with the pathogenic SIV/DeltaB670 isolate (18). Axillary LNs were examined from acutely infected (2 wk PI) and AIDS-developing (defined by decreasing CD4 counts, opportunistic infections, and wasting) animals, as well as uninfected controls (Table I). Because FOXP3 is considered to be a highly specific marker for T_{reg} (3), changes in its expression were measured at the RNA and protein levels. FOXP3 mRNA levels in LNs were decreased both early and late after SIV infection (Fig. 1A). Immunofluorescence staining for FOXP3⁺ cells in LN tissue sections also revealed a 60–70% decrease in the proportion of cells that were FOXP3⁺ after SIV infection (Fig. 1, B and C), which was highly correlated with the mRNA measurements (*r* = 0.721, *p* = 0.008). Additionally, flow cytometric analyses of LN single-cell suspensions confirmed an ~50% decrease in the FOXP3⁺ proportion of total live cells following SIV infection (Fig. 1D). These findings indicate there was a loss of FOXP3⁺ T_{reg} in LNs after pathogenic SIV infection of cynomolgus macaques.

The cytokine TGF- β 1 is expressed by T_{reg}, acts in concert with IL-2 in the differentiation and survival of inducible T_{reg} (4) and suppresses IFN- γ expression (22). Measurement of TGF- β 1 and IL-2 mRNA levels in macaque LNs indicated that they also were decreased following SIV infection (Fig. 1, E and F), and were highly correlated with FOXP3 levels (Fig. 1G; *r* = 0.91).

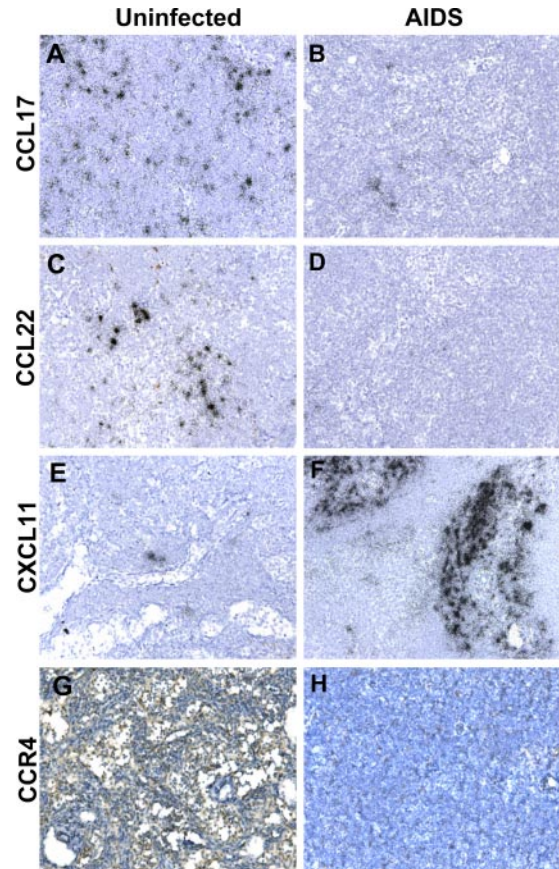


FIGURE 3. In situ detection of chemokine and chemokine receptor levels in axillary LN tissue sections from SIV-infected and uninfected cynomolgus macaques. *A–F*, In situ hybridization was performed for the indicated chemokine mRNA in axillary LN tissue sections from uninfected or AIDS-developing macaques. Parallel hybridization of tissue sections with the cognate sense control probe provided no specific in situ hybridization signal (data not shown). Immunohistochemical staining was performed with a polyclonal antiserum for CCR4 (*G, H*). Original magnifications, $\times 200$.

Decreased expression of TGF- β 1 and IL-2 could contribute to the reduction in FOXP3⁺ T_{reg} levels in LNs during SIV infection by reducing differentiation of naive T cells into inducible T_{reg}. Although there were decreases in FOXP3, TGF- β 1, and IL-10 (data not shown) expression, another immunosuppressive element, IDO was significantly increased after SIV infection, as was IFN- γ , an upstream inducer of IDO (23) (Fig. 1, *H* and *I*). This is consistent with reports that IDO is increased in tonsils of HIV-1-infected patients (24) and LNs of SIV-infected rhesus macaques (16).

Loss of T_{reg} would be expected to lead to increased immune activation and this was observed. Immunofluorescence detection and enumeration of CD3⁺ cells also positive for the proliferation marker Ki67 in macaque LNs revealed that the percentage of CD3⁺ cells that was also Ki67⁺ increased 3- to 5-fold after SIV infection (Fig. 1J). Overall proportions of Ki67⁺ cells were also significantly increased after SIV infection (data not shown). These data indicated that T cell activation levels increased concordantly with loss of T_{reg}.

Human T_{reg} highly express CCR4 (7) and CCR7 (5), and thus their ligands CCL17 and CCL21 could modulate homing of T_{reg} to lymphoid tissues. Measurement of mRNA levels of these and other chemokines in macaque LNs revealed that mRNAs encoding ligands for CCR4 (CCL17 and CCL22) and CCR7

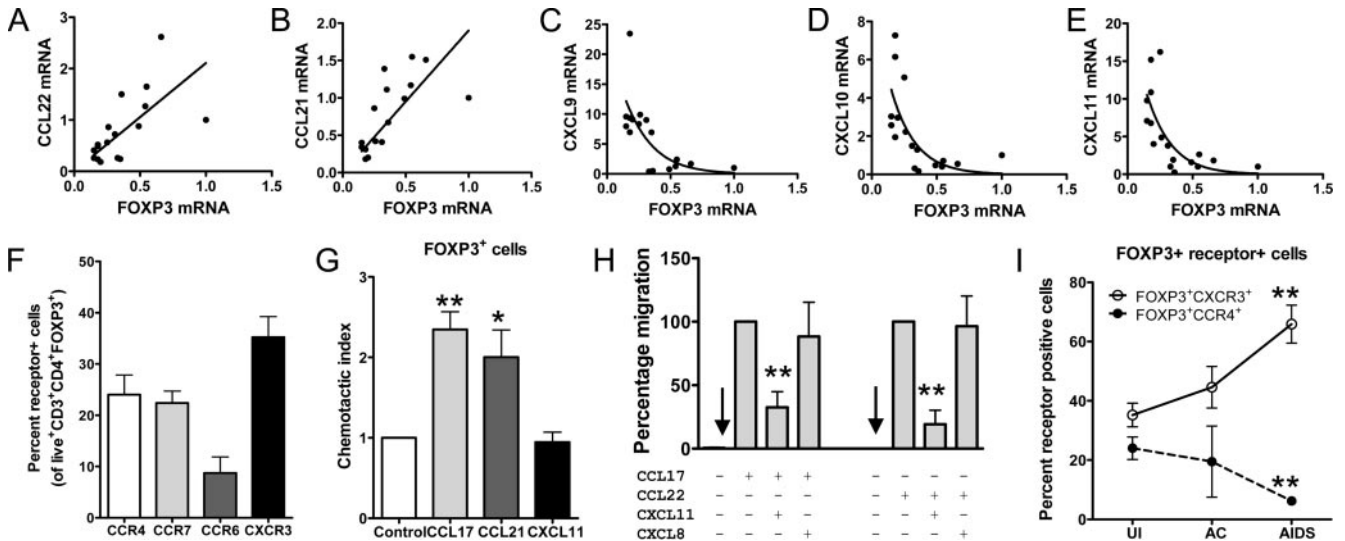


FIGURE 4. Association between CXCR3 ligand and CCR4 ligand expression and function and FOXP3 levels in macaque LNs. Linear (*A* and *B*) and nonlinear (*C–E*) regression analysis plots of FOXP3 mRNA vs the indicated chemokine mRNA levels are shown. *F*, Flow cytometry was used to detect chemokine receptor expression on live⁺CD3⁺CD4⁺FOXP3⁺ axillary LN cells from uninfected ($n = 5$) cynomolgus macaques. *G*, Axillary LN cells from uninfected macaques ($n = 4$ macaques) were subjected to chemotaxis to the indicated chemokines and immunocytochemical staining for FOXP3⁺ was performed on the migrated cells. The chemotactic indices were calculated as the fraction of FOXP3⁺ cells in the migrated population relative to the input cells. *, $p < 0.05$ and **, $p < 0.01$. *H*, The migration of cells stably expressing CCR4 in response to CCL17 (10 nM) or CCL22 (10 nM) was examined in the presence or absence of 1 μ M CXCL11 or CXCL8 antagonist. The percentage of cells migrating was calculated relative to migration toward CCL17 or CCL22 alone. The data represent the mean \pm SEM of four independent experiments. **, $p < 0.01$, compared with agonist alone. *I*, The percentages of live⁺CD3⁺CD4⁺FOXP3⁺ cells expressing either CXCR3 or CCR4, as determined by flow cytometry, are shown as a function of disease state.

(CCL21) decreased (Fig. 2, *A–C*) following SIV infection, whereas mRNAs encoding IFN- γ -inducible CXCR3 ligands (CXCL9–11) increased (Fig. 2, *D–F*). The expression levels of the cognate chemokine receptors changed in parallel with their respective ligands (Fig. 2, *G–I*). The changes in CCR4 and CXCR3 ligand expression were likely driven by the increased IFN- γ levels (Fig. 1*I*), because *ex vivo* treatment of macaque LN cells with IFN- γ led to simultaneous induction of CXCR3 ligands and decrease of CCR4 ligands (Fig. 2, *J* and *K*). Correlation analyses revealed that in LNs, levels of CCL17 and CCL22 were positively correlated with those of their receptor CCR4 ($r = 0.761$ and $r = 0.736$, respectively), and levels of CCL21 were positively correlated with CCR7 ($r = 0.646$). In situ hybridization and immunostaining of tissue sections confirmed these changes in chemokine and chemokine receptor expression primarily in paracortical regions (Fig. 3).

More extensive correlation analyses revealed that FOXP3 mRNA levels were positively correlated with CCL22 ($r = 0.627$) and CCL21 ($r = 0.682$) levels (Fig. 4, *A* and *B*) and their cognate receptors CCR4 ($r = 0.493$) and CCR7 ($r = 0.745$), respectively, but negatively correlated with CXCL9 ($r = -0.615$), CXCL10 ($r = -0.552$), and CXCL11 ($r = -0.584$) levels (Fig. 4, *C–E*) and local SIV viral RNA loads ($r = -0.735$). These findings indicate that loss of T_{reg} in macaque LNs during SIV infection is associated with multiple changes in chemokine, cytokine and SIV levels.

Given that CCR4 and CCR7 are expressed by a large proportion of T_{reg} (7) and have been shown to be important in T_{reg} homing to LNs and other tissues (5, 6), we used flow cytometry to examine their expression on FOXP3⁺ cells in uninfected macaque LNs, the strategy of which is outlined in Fig. 5. Approximately 25% of CD3⁺CD4⁺FOXP3⁺ cells expressed CCR4 or CCR7 (Fig. 4*F*), whereas 35% expressed CXCR3 and 10% expressed CCR6. To determine whether CCL17, CCL21,

and CXCL11 recruit FOXP3⁺ cells via CCR4, CCR7, and CXCR3, respectively, we performed chemotaxis with uninfected macaque LN cells. Immunostaining of FOXP3 in the input and migrated cells revealed that CCL17 and CCL21 recruited a population of cells that had a greater proportion of FOXP3⁺ cells than that recruited by CXCL11 (Fig. 4*G*), despite clear expression of CXCR3 (Fig. 4*F*). The lack of recruitment by CXCL11 could represent the net effect of positive and negative signaling through different receptors or possibly uncoupling of CXCR3 at the intracellular interface (25). These chemotactic data support the interpretation that CCL17 and CCL21 contribute to homing of FOXP3⁺ T_{reg} into LNs and the reduced expression of these chemokines (Fig. 2) could contribute to loss or redistribution of FOXP3⁺ cells after SIV infection.

Given that ligands for CXCR3 antagonize the type 2 chemokine receptor CCR3 (26) and are up-regulated during SIV infection (Fig. 2), we examined whether a CXCR3 ligand would antagonize the type 2 and T_{reg} chemokine receptor CCR4. The migration of cells stably expressing CCR4 in response to CCL17 or CCL22 was inhibited by a 100-fold excess of CXCL11 (Fig. 4*H*), whereas 100-fold excess of the CXCR2 ligand CXCL8 did not antagonize CCR4. CXCL11 alone did not induce chemotaxis of the CCR4⁺ cells (data not shown). Therefore, simultaneous antagonism of CCR4 by increased CXCR3 ligand expression and loss of CCR4 ligand expression could contribute to reduced homing of FOXP3⁺ cells to LNs during SIV infection. The nonlinear, negative correlations between CXCR3 ligand and FOXP3 levels (Fig. 4, *C–E*) indicate that even moderate changes in the CXCR3 ligand expression are likely to have potent inhibitory effects on homing of FOXP3⁺ T_{reg} to LNs. Finally, consistent with the antagonism of CCR4 by CXCR3 ligands, the proportion of T_{reg}-expressing CCR4 in macaque LNs decreased during the course of SIV infection (Fig. 4*I*).

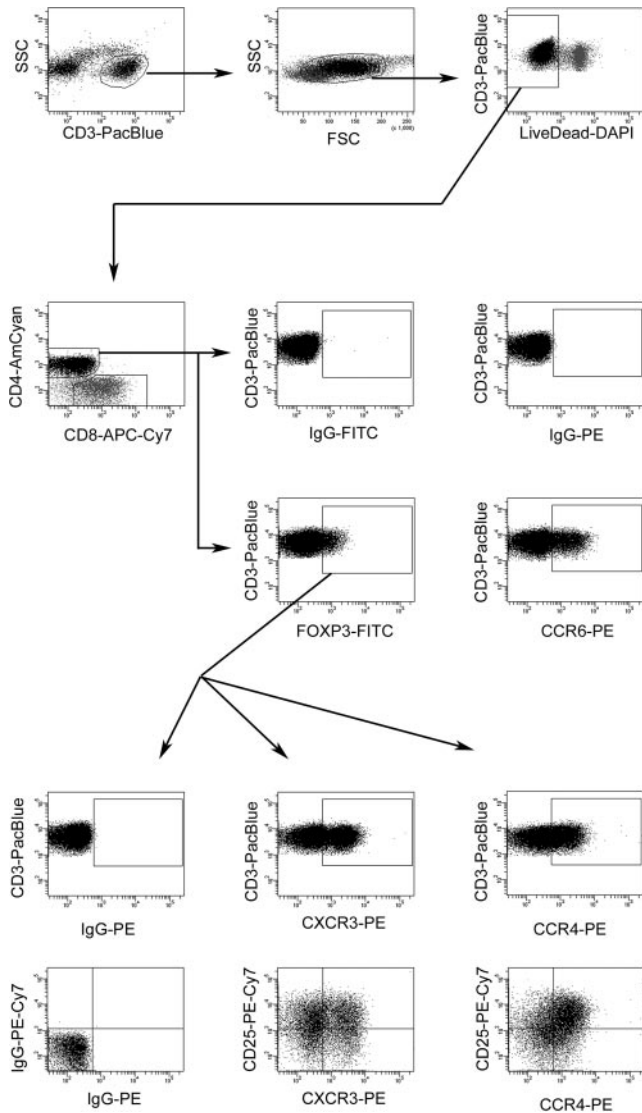


FIGURE 5. Flow cytometric gating strategy used to measure chemokine receptor expression on macaque FOXP3⁺CD4⁺ T lymphocytes. Shown is the successive gating strategy used to ultimately visualize chemokine receptor levels on cynomolgus macaque LN T_{reg}. Details are described in *Materials and Methods*.

Discussion

In the present study, we found that FOXP3⁺ cells are lost early during pathogenic SIV infection and with loss evident also during AIDS, which is consistent with recent findings in rhesus macaques (15). This loss of T_{reg} was correlated with increased levels of local cellular activation and could be a key mechanism in the cumulative loss of immune function culminating in AIDS. In addition, we have identified multiple chemokine- and cytokine-mediated mechanisms that can account for the loss in T_{reg} in SIV-infected macaques.

In contrast to our findings, other recent studies have reported that rhesus macaques acutely and chronically infected with SIVmac251 (16, 17) and humans infected with HIV-1 (17, 24) had increased FOXP3⁺ T_{reg} levels and TGF-β1 expression in lymphoid tissues. These differences could be due to the different host systems studied, different viral strains, and different SIV inoculation routes, although our preliminary examination of rhesus macaque LNs following SIV/DeltaB670 infection also revealed a loss of T_{reg} (data not shown). Another explanation might be due to

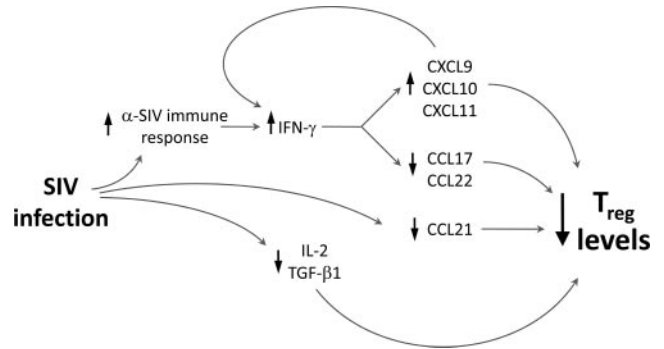


FIGURE 6. Model for chemokine- and cytokine-mediated loss of T_{reg} in macaque LNs. Shown schematically are the relationships between IFN-γ-driven changes in CXCR3 and CCR4 ligand expression and IL-2/TGF-β1-driven differentiation of T_{reg} on overall T_{reg} levels in LNs following SIV infection as detailed in *Discussion*. The arrows pointing up or down next to each component indicate the positive or negative effects of upstream players on the levels of the component.

variation in the timing of the contraction and/or expansion of T_{reg} frequencies, as shown by Pereira et al. (15) in longitudinal studies of SIVmac239-infected rhesus macaques. In this study, the proportion of T_{reg} among CD4⁺ T cells decreased in LN and intestinal tissues of SIVmac239-infected rhesus macaques, but not in naturally infected sootey mangabey monkeys. Perhaps there are multiple avenues leading to the development of AIDS and, during HIV-1 or SIV infection, loss of T_{reg} or expansion of T_{reg} could represent separate paths that both ultimately contribute to the development of immunodeficiency when threshold levels are crossed. Loss of T_{reg} would lead to T cell hyperactivation and enhance HIV-1 and SIV replication and activation-associated cell death, whereas expansion of T_{reg} could lead to suppression of HIV-1-specific and other immune responses.

In this study, we have identified multiple, previously unrecognized mechanisms for the loss of T_{reg} during pathogenic SIV infection of cynomolgus macaques. Given that we found FOXP3 mRNA and protein levels decreased in LNs during SIV infection and FOXP3 mRNA levels were negatively correlated with local SIV viral loads, SIV infection has a role in the decline in T_{reg} in macaque LNs, perhaps through infection of these cells (27). In addition, our findings support three additional mechanisms contributing to this SIV-driven loss of T_{reg}, which are outlined schematically in Fig. 6. First, reduced levels of TGF-β1 and IL-2 will lead to fewer naive T cells being differentiated into inducible T_{reg} (4). Second, reduced levels of CCR4 and CCR7 ligands, associated with increased IFN-γ levels, will lead to decreased recruitment of CCR4⁺ and/or CCR7⁺ T_{reg} into lymphoid tissues. Finally, potent up-regulation of CXCR3 ligand expression will provide abundant natural CCR4 antagonists that will also reduce recruitment of CCR4⁺ cells, including T_{reg}. The intriguing sensitivity of FOXP3 levels to CXCR3 ligand levels as observed through regression analyses, supports their central role in loss of T_{reg} in macaque LNs. The increase of IFN-γ as an upstream regulator of CXCR3 ligand expression and the decrease in TGF-β1 as an upstream regulator of IFN-γ expression (22) reveal a complex set of interrelationships that control multiple positive and negative feedback systems.

Decline in T_{reg} numbers in LNs during SIV infection would reduce suppression of conventional T cells, contribute to their activation, and thereby provide enhanced opportunities for HIV-1 and SIV replication by modulating the composition and availability of cellular substrates. One hallmark of HIV-1 infection is immune activation (28), and loss of T_{reg}, and TGF-β1 and IL-10

expression, offer mechanisms by which this might occur. Non-pathogenic SIV infections in African green monkeys (13, 29) and sootey mangabeys have been shown not to increase cellular activation despite substantial viral replication. Consistent with our findings linking loss of T_{reg} with increased immune activation during pathogenic SIV infection, naturally infected nonhuman primates do not show a loss of T_{reg} (15). Increased activation in pathogenic SIV infections will provide cellular substrates and an environment that will sustain viral replication and lead to greater loss of immune function through direct and indirect killing as well as activation-induced cell death. Our data indicate that T cell activation levels increased concordantly with loss of T_{reg}, consistent with the role of T_{reg} in balancing overall local levels of cellular activation. In addition, another disease outcome likely linked to loss of T_{reg} is the reported increase in susceptibility to autoimmune and inflammatory diseases in some HIV-1-infected individuals (30). Overall, our findings have revealed a complex set of changes in chemokine and cytokine expression during pathogenic SIV infection that lead to concomitant loss of T_{reg}. Modulating the trafficking, induction, or survival of these cells through strategies targeting chemokine receptors or retinoic acid pathways (31) might represent new approaches for treating HIV-1 infected individuals.

Acknowledgments

We thank Dr. Velpandi Ayyavoo for critically reading this manuscript, Dr. Ashley Haase for insightful discussion and sharing advice on FOXP3 staining of tissue sections, and Melanie Pfeifer for assistance with generation of macaque LN single-cell suspensions.

Disclosures

The authors have no financial conflict of interest.

References

- Sakaguchi, S., M. Ono, R. Setoguchi, H. Yagi, S. Hori, Z. Fehervari, J. Shimizu, T. Takahashi, and T. Nomura. 2006. Foxp3⁺CD25⁺CD4⁺ natural regulatory T cells in dominant self-tolerance and autoimmune disease. *Immunol. Rev.* 212: 8–27.
- Suvas, S., U. Kumaraguru, C. D. Pack, S. Lee, and B. T. Rouse. 2003. CD4⁺CD25⁺ T cells regulate virus-specific primary and memory CD8⁺ T cell responses. *J. Exp. Med.* 198: 889–901.
- Hori, S., T. Nomura, and S. Sakaguchi. 2003. Control of regulatory T cell development by the transcription factor Foxp3. *Science* 299: 1057–1061.
- Zheng, S. G., J. Wang, P. Wang, J. D. Gray, and D. A. Horwitz. 2007. IL-2 is essential for TGF- β to convert naive CD4⁺CD25⁻ cells to CD25⁺Foxp3⁺ regulatory T cells and for expansion of these cells. *J. Immunol.* 178: 2018–2027.
- Schneider, M. A., J. G. Meingassner, M. Lipp, H. D. Moore, and A. Rot. 2007. CCR7 is required for the in vivo function of CD4⁺CD25⁺ regulatory T cells. *J. Exp. Med.* 204: 735–745.
- Sather, B. D., P. Treuting, N. Perdue, M. Miazgowiec, J. D. Fontenot, A. Y. Rudensky, and D. J. Campbell. 2007. Altering the distribution of Foxp3⁺ regulatory T cells results in tissue-specific inflammatory disease. *J. Exp. Med.* 204: 1335–1347.
- Lim, H. W., H. E. Broxmeyer, and C. H. Kim. 2006. Regulation of trafficking receptor expression in human forkhead box P3⁺ regulatory T cells. *J. Immunol.* 177: 840–851.
- Reinhart, T. A., B. A. Fallert, M. E. Pfeifer, S. Sanghavi, S. Capuano, III, P. Rajakumar, M. Murphey-Corb, R. Day, C. L. Fuller, and T. M. Schaefer. 2002. Increased expression of the inflammatory chemokine CXC chemokine ligand 9/monokine induced by interferon- γ in lymphoid tissues of rhesus macaques during simian immunodeficiency virus infection and acquired immunodeficiency syndrome. *Blood* 99: 3119–3128.
- LaFranco-Scheuch, L., K. Abel, N. Makori, K. Rothausler, and C. J. Miller. 2004. High β -chemokine expression levels in lymphoid tissues of simian/human immunodeficiency virus 89.6-vaccinated rhesus macaques are associated with uncontrolled replication of simian immunodeficiency virus challenge inoculum. *J. Virol.* 78: 6399–6408.
- Grossman, Z., M. Meier-Schellersheim, A. E. Sousa, R. M. M. Victorino, and W. E. Paul. 2002. CD4⁺ T-cell depletion in HIV infection: are we closer to understanding the cause? *Nat. Med.* 8: 319–323.
- Sempere, J. M., V. Soriano, and J. M. Benito. 2007. T regulatory cells and HIV infection. *AIDS Rev.* 9: 54–60.
- Rouse, B. T., P. P. Sarangi, and S. Suvas. 2006. Regulatory T cells in virus infections. *Immunol. Rev.* 212: 272–286.
- Kornfeld, C., M. J. Ploquin, I. Pandrea, A. Faye, R. Onanga, C. Apetrei, V. Poaty-Mavoungou, P. Rouquet, J. Estaquier, L. Mortara, et al. 2005. Anti-inflammatory profiles during primary SIV infection in African green monkeys are associated with protection against AIDS. *J. Clin. Invest.* 115: 1082–1091.
- Eggena, M. P., B. Barugahare, N. Jones, M. Okello, S. Mutalya, C. Kityo, P. Mugenyi, and H. Cao. 2005. Depletion of regulatory T cells in HIV infection is associated with immune activation. *J. Immunol.* 174: 4407–4414.
- Pereira, L. E., F. Villinger, N. Onlamoon, P. Bryan, A. Cardona, K. Pattanapanyasat, K. Mori, S. Hagen, L. Picker, and A. A. Ansari. 2007. Simian immunodeficiency virus (SIV) infection influences the level and function of regulatory T cells in SIV-infected rhesus macaques but not SIV-infected sooty mangabeys. *J. Virol.* 81: 4445–4456.
- Estes, J. D., Q. Li, M. R. Reynolds, S. Wietgrefe, L. Duan, T. Schacker, L. J. Picker, D. I. Watkins, J. D. Lifson, C. Reilly, et al. 2006. Premature induction of an immunosuppressive regulatory T cell response during acute simian immunodeficiency virus infection. *J. Infect. Dis.* 193: 703–712.
- Nilsson, J., A. Boasso, P. A. Velilla, R. Zhang, M. Vaccari, G. Franchini, G. M. Shearer, J. Andersson, and C. Chougnnet. 2006. HIV-1-driven regulatory T-cell accumulation in lymphoid tissues is associated with disease progression in HIV/AIDS. *Blood* 108: 3808–3817.
- Murphey-Corb, M., L. N. Martin, S. R. Rangan, G. B. Baskin, B. J. Gormus, R. H. Wolf, W. A. Andes, M. West, and R. C. Montelaro. 1986. Isolation of an HTLV-III-related retrovirus from macaques with simian AIDS and its possible origin in asymptomatic mangabeys. *Nature* 321: 435–437.
- Sanghavi, S. K., and T. A. Reinhart. 2005. Increased expression of TLR3 in lymph nodes during simian immunodeficiency virus infection: implications for inflammation and immunodeficiency. *J. Immunol.* 175: 5314–5323.
- Godfrey, T. E., S. H. Kim, M. Chavira, D. W. Ruff, R. S. Warren, J. W. Gray, and R. H. Jensen. 2000. Quantitative mRNA expression analysis from formalin-fixed, paraffin-embedded tissues using 5' nuclease quantitative reverse transcription-polymerase chain reaction. *J. Mol. Diagn.* 2: 84–91.
- Fox, J. M., P. Najarro, G. L. Smith, S. Struyf, P. Proost, and J. E. Pease. 2006. Structure/function relationships of CCR8 agonists and antagonists: amino-terminal extension of CCL1 by a single amino acid generates a partial agonist. *J. Biol. Chem.* 281: 36652–36661.
- Lin, J. T., S. L. Martin, L. Xia, and J. D. Gorham. 2005. TGF- β 1 uses distinct mechanisms to inhibit IFN- γ expression in CD4⁺ T cells at priming and at recall: differential involvement of Stat4 and T-bet. *J. Immunol.* 174: 5950–5958.
- Sarkar, S. A., R. Wong, S. I. Hackl, O. Mousa, R. G. Gill, A. Wiseman, H. W. Davidson, and J. C. Hutton. 2007. Induction of indoleamine 2,3-dioxygenase by interferon- γ in human islets. *Diabetes* 56: 72–79.
- Anderson, J., A. Boasso, J. Nilsson, R. Zhang, N. J. Shire, S. Lindback, G. M. Shearer, and C. A. Chougnnet. 2005. The prevalence of regulatory T cells in lymphoid tissue is correlated with viral load in HIV-infected patients. *J. Immunol.* 174: 3143–3147.
- Thompson, B. D., Y. Jin, K. H. Wu, R. A. Colvin, A. D. Luster, L. Birnbaumer, and M. X. Wu. 2007. Inhibition of G α i2 activation by G α i3 in CXCR3-mediated signaling. *J. Biol. Chem.* 282: 9547–9555.
- Xanthis, G., C. E. Duchesnes, T. J. Williams, and J. E. Pease. 2003. CCR3 functional responses are regulated by both CXCR3 and its ligands CXCL9, CXCL10, and CXCL11. *Eur. J. Immunol.* 33: 2241–2250.
- Oswald-Richter, K., S. M. Grill, N. Shariat, M. Leelawong, M. S. Sundrud, D. W. Haas, and D. Unutmaz. 2004. HIV infection of naturally occurring and genetically reprogrammed human regulatory T-cells. *PLoS Biol.* 2: 955–966.
- Hazenberg, M. D., S. A. Otto, B. H. van Benthem, M. T. Roos, R. A. Coutinho, J. M. Lange, D. Hamann, M. Prins, and F. Miedema. 2003. Persistent immune activation in HIV-1 infection is associated with progression to AIDS. *AIDS* 17: 1881–1888.
- Silvestri, G., D. L. Sodora, R. A. Koup, M. Paiardini, S. P. O'Neil, H. M. McClure, S. I. Staprans, and M. B. Feinberg. 2003. Nonpathogenic SIV infection of sooty mangabeys is characterized by limited bystander immunopathology despite chronic high-level viremia. *Immunity* 18: 441–452.
- Zandman-Goddard, G., and Y. Shoenfeld. 2002. HIV and autoimmunity. *Autoimmun. Rev.* 1: 329–337.
- Coombes, J. L., K. R. Siddiqui, C. V. Rancibia-Carcamo, J. Hall, C. M. Sun, Y. Belkaid, and F. Powrie. 2007. A functionally specialized population of mucosal CD103⁺ DCs induces Foxp3⁺ regulatory T cells via a TGF- β and retinoic acid-dependent mechanism. *J. Exp. Med.* 204: 1757–1764.